

## Article

# FLUS Based Modeling of the Urban LULC in Arid and Semi-Arid Region of Northwest China: A Case Study of Urumqi City

Yusuyunjiang Mamitimin <sup>1,2,\*</sup>, Zibibula Simayi <sup>1,2</sup>, Ayinuer Mamat <sup>3</sup> , Bumairiyemu Maimaiti <sup>4</sup> and Yunfei Ma <sup>1,2</sup><sup>1</sup> College of Geography and Remote Sensing Sciences, Xinjiang University, Urumqi 830017, China<sup>2</sup> Key Laboratory of Smart City and Environment Modeling of Higher Education Institute, Urumqi 830017, China<sup>3</sup> Kashgar Satellite Data Receiving Ground Station, Aerospace Information Research Institute, Chinese Academy of Sciences, Kashgar 844000, China<sup>4</sup> College of Public Management (Law), Xinjiang Agricultural University, Urumqi 830052, China

\* Correspondence: y\_mamitimin@163.com; Tel.: +86-15276862217

**Abstract:** Modeling land use and land cover (LULC) change is important for understanding its spatiotemporal trends and plays a crucial role in land use planning and natural resources management. To this end, this study assessed the spatiotemporal characteristics of the LULC changes in Urumqi city between 1980 and 2020. In addition, future LULC was successfully projected for 2030 and 2050 under different scenarios based on the FLUS model. This model was validated using actual and simulated land use data for 2020. The kappa coefficient and figure of merit of the simulation results for 2020 were 0.87 and 0.114, respectively, indicating that the simulation accuracy was satisfactory. The results demonstrated that grassland was the major land use type, with the area accounting for more than 50% of the study area. From 1980 to 2020, urban land greatly expanded, while grassland decreased significantly. Urban land increased from 353.51 km<sup>2</sup> to 884.27 km<sup>2</sup>, while grassland decreased from 7903.4 km<sup>2</sup> to 7414.92 km<sup>2</sup> from 1980 to 2020. In addition, significant transitions mainly occurred between grasslands, cultivated lands and urban lands. Grassland and cultivated land were converted into urban land, resulting in rapid urban expansion over the last 40 years. From 1990 to 2000, grassland was converted into urban land with an area of 341.08 km<sup>2</sup>. Finally, the simulation results of the LULC showed that urban land is expected to increase under all three scenarios, and cultivated land, grassland and forest land are effectively protected under the Cultivated Land Protection Scenario (CPS) and Ecological Protection Scenario (EPS) compared to the Baseline Scenario (BLS). This study assessed the spatiotemporal characteristics and transitions of LULC between 1980 and 2020, and successfully projected LULC for 2035 and 2050 in Urumqi City in the arid and semi-arid regions of northwest China based on the FLUS model, which has not been investigated in previous studies.



**Citation:** Mamitimin, Y.; Simayi, Z.; Mamat, A.; Maimaiti, B.; Ma, Y. FLUS Based Modeling of the Urban LULC in Arid and Semi-Arid Region of Northwest China: A Case Study of Urumqi City. *Sustainability* **2023**, *15*, 4912. <https://doi.org/10.3390/su15064912>

Academic Editors: Alimujiang Kasimu and Liwei Zhang

Received: 7 February 2023

Revised: 7 March 2023

Accepted: 7 March 2023

Published: 9 March 2023



**Copyright:** © 2023 by the authors. Licensee MDPI, Basel, Switzerland. This article is an open access article distributed under the terms and conditions of the Creative Commons Attribution (CC BY) license (<https://creativecommons.org/licenses/by/4.0/>).

**Keywords:** LULC; arid region; FLUS model; urbanization

## 1. Introduction

Urbanization is an inevitable trend of social development and has become one of the most important changes in human society since the 20th century [1]. According to the *World Urbanization Prospects: The 2018 Revision* released by the United Nations Population Division, the proportion of the world's urban population reached 55% in 2018 and it is expected to reach 68% by 2050 [2]. Rapid urbanization has not only changed the urban landscape, but has also greatly improved the living conditions, public services and urban infrastructure available for residents. However, the continuous expansion of industrial and residential areas resulting from rapid urbanization has aggravated the shortage of land resources and unreasonable utilization [3–5], as well as changed the hydrological systems of cities by reducing the available permeable surface [6]. Additionally, other problems, such

as ecological destruction, environmental pollution and traffic congestion, are becoming more prominent with the acceleration of urbanization [7–9]. Therefore, understanding the spatiotemporal changes and predicting future LULCs are essential to ensure sustainable land management meets the increasing pressures of basic human needs and protects the environment and natural resources.

The LULC modeling technique is an effective tool for understanding spatiotemporal trends, which helps policy makers to implement necessary measures and sustainably protect valuable land resources [10]. Accurate modeling can enhance the understanding of land use change processes and driving factors and can also predict alternative land use scenarios that may lead to sustainable development goals. Many models and software packages are available and widely used in future land use simulations under different scenarios, including the Conversion of Land Use and its Effects at Small Region Extents (CLUE-S) model [11–14], the Patch-Generating Land Use Simulation (PLUS) model [15,16], the Future Land Use Simulation (FLUS) model [17–19], the Land Change Modeler (LCM) [20] and the CA-Markov model [21,22]. Among these models, the FLUS model is frequently applied in urban land use simulations owing to its simplicity and bottom-up approach. The FLUS model has been successfully applied to land use simulation in many cities in China, including Wuhan [23,24], Guangzhou [25,26] and Chongqing [27]. The results of these studies showed that the FLUS model can simulate the future LULC with a high degree of accuracy. However, all these studies focused on the cities in eastern China, and limited research has been conducted in cities in the arid and semi-arid regions of northwest China.

Urumqi, located in the center of the Eurasian continent, is the capital of Xinjiang Uygur Autonomous Region. It is not only the political, economic and cultural center of Xinjiang Uygur Autonomous Region, but also the important transportation hub of China's "Belt and Road" initiative. Additionally, Urumqi City is a typical oasis city characterized by a temperate continental climate, which is completely different from most other Chinese cities. Over the last 40 years, the urbanization process of Urumqi has accelerated. Rapid urbanization not only causes a series of ecological and environmental problems, but also puts great pressure on land resources. Therefore, understanding the spatiotemporal changes and predicting future LULC in Urumqi City is essential for the rational allocation of land resources. The objectives of the study were to: (1) assess the spatiotemporal characteristics of the LULC from 1980 to 2020 in Urumqi City in the arid and semi-arid regions of northwest China; (2) analyze the transitions in LULC from 1980 to 2020; and (3) simulate the future LULC for 2030 and 2050 under different scenarios based on the FLUS model. The results of this study may provide information on the LULC change hand scientific evidence for land use planning and natural resources management.

## 2. Materials and Methods

### 2.1. Study Area

Urumqi (86°37'–88°58' E, 42°45'–44°08' N), the capital city of Xinjiang Uyghur Autonomous Region, is located on the northern slope of the Tianshan Mountains and the southern edge of the Junggar Basin (Figure 1). Being far from the ocean and surrounded by mountains, the study area is characterized by a typical temperate continental climate. The annual average temperature is 7.3 °C, while the annual average precipitation is 236 mm [28]. Urumqi City includes seven districts and one county with a total area of 14,200 km<sup>2</sup>. According to the official statistical data, the population of Urumqi City was found to be 2.22 million, of which the urban population was 2.003 million with the urbanization rate of 90.2% at the end of 2018, and the average annual natural growth rate of the total population between 1980 and 2018 was 2.28%.

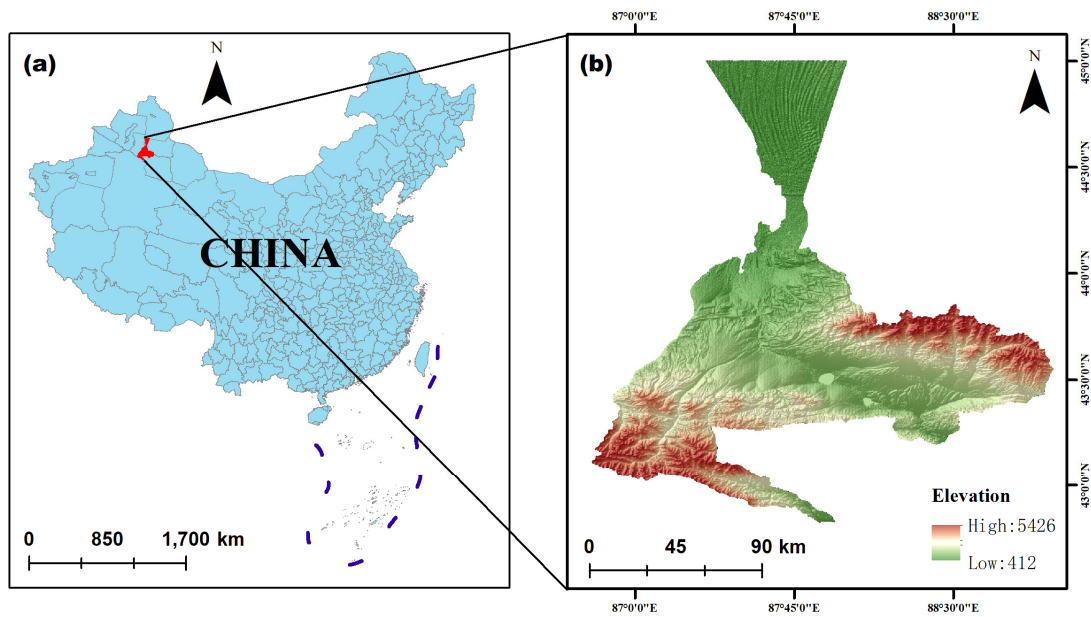


**Figure 1.** Geographic location (a) and topographic map (b) of the study area.

## 2.2. Data Source and Processing

The LULC dataset was obtained from the Data Center for Resources and Environmental Sciences, Chinese Academy of Sciences (RESDC), with a spatial resolution of  $30\text{ m} \times 30\text{ m}$  (<https://www.resdc.cn>, accessed on 25 October 2021). The LULC data for 1980, 1990 and 2000 were interpreted based on the LANDSAT TM/ETM remote sensing images, while the LULC data for 2010 and 2020 were based on the LANDSAT 8 OLI remote sensing images. The overall accuracy of the interpretation of the datasets were reported to be above 90% for the entire time period. The LULC data were reclassified into six types: cultivated land, forest land, grassland, water bodies, urban land and unused land. The Digital Elevation Model (DEM) was obtained from the Geospatial Data Cloud site, Computer Network Information Center, Chinese Academy of Sciences (<http://www.gscloud.cn>, accessed on 10 April 2022), and a slope map was generated using the slope module of ArcGIS 10.3 based on the DEM data. Vector data of transportation networks and settlements were collected from the National Platform for Common Geospatial Information Services of China (<https://www.tianditu.gov.cn>, accessed on 12 August 2022), and proximity to human settlements, proximity to highways, proximity to other roads and proximity to railway were calculated using the Euclidean distance module of ArcGIS 10.3. All data, including reprojection and resampling, were pre-processed, because the data were obtained from the various sources with different coordinate systems and spatial resolutions.

## 2.3. FLUS Model

The FLUS (Future Land Use Simulation) model was used to simulate future land use in the study region. The FLUS model is based on the principle of cellular automata (CA) and introduces an artificial neural network (ANN) algorithm that can obtain the suitability probability of various types of changes according to the initial land use and various drivers. The prediction task integrates the ANN algorithm with the CA and Markov Chain models. An ANN is a nonparametric machine learning technique used to quantify and model complex behaviors and patterns [29]. The neural network structure includes an input layer, one or more hidden layers—each with a different number of neurons—and an output layer that stores the predicted value [30]. Establishing the relationship between the initial land use type and the spatial effects of various driving factors is the main simulation process of the neural network, which can be written as:

$$p(p, k, t) = \sum_j w_{j,k} \times \text{sigmoid}(\text{net}_j(p, t)) \quad (1)$$

$$\text{sigmoid}(net_j(p, t)) = \frac{1}{1 + e^{-net_j(p, t)}} \quad (2)$$

$$net_j(p, t) = \sum w_{i,j} \times c \quad (3)$$

$p(p, k, t)$  represents the occurrence probability of land use type  $k$  at the grid  $p$  and time  $t$ , and  $w_{j,k}$  represents the weight between the output and the hidden layers.  $\text{sigmoid}(net_j(p, t))$  represents the association function from the hidden layer to the output layer, whereas  $net_j(p, t)$  represents the signal sent by the hidden layer  $j$  to neuron  $j$  at the grid  $p$  and time  $t$ .  $w_{i,j}$  represents the signal between the input and hidden layers.

The CA model has a strong ability to simulate the spatiotemporal characteristics of complex systems [31]. The CA model can provide insights into local and global patterns of land use and land cover dynamics that link new states to their previous and neighboring states [32,33]. Most importantly, as an analytical engine, the CA model supports dynamic modeling in GIS and remote sensing environments [34,35]. The mathematical expression can be written as [36]:

$$S(t, t + 1) = f(s(t), N) \quad (4)$$

where  $S$  represents the cellular states, while  $N$  represents the cellular field,  $t, t + 1$  represents the different times and  $f$  is the rule of the transformation for cellular states.

A Markov chain (MC) is a random process describing a sequence of events in which future events depend only on current and previous events without considering the history of the entire event [37]. Predicted future LULC changes depend on the probability of subsequent transitions created from past or current LULC changes [38]. However, one of the limitations is that the MC model only predicts the quantity of the LULC changes and cannot provide the spatial distribution of the LULC changes [39]. Hence, many studies have applied hybrid models that integrate the MC and CA models for future land use simulations. The mathematical expression can be written as [40,41]:

$$S_{(t+1)} = P_{ij} \times S_{(t)} \quad (5)$$

$$P_{ij} = \begin{bmatrix} p_{11} & \cdots & p_{1n} \\ \vdots & \ddots & \vdots \\ p_{n1} & \cdots & p_{nn} \end{bmatrix} \quad (6)$$

where  $P_{ij}$  represents the probability matrix of transition, while  $i$  and  $j$  represent the LULC type at the time of  $t$  and  $t+1$ ,  $n$  is the number of LULC types and  $S_{(t)}$  and  $S_{(t+1)}$  are the status of the LULC at the time of  $t$  and  $t+1$ .

#### 2.4. Selection of the Driving Factors

LULC is a complex system and process that is affected by natural, socioeconomic and accessibility factors. According to the existing studies on the LULC driving mechanism, six factors including elevation, slope, proximity to human settlement, proximity to highway, proximity to other roads and proximity to railroad were selected in this study (Figure 2).

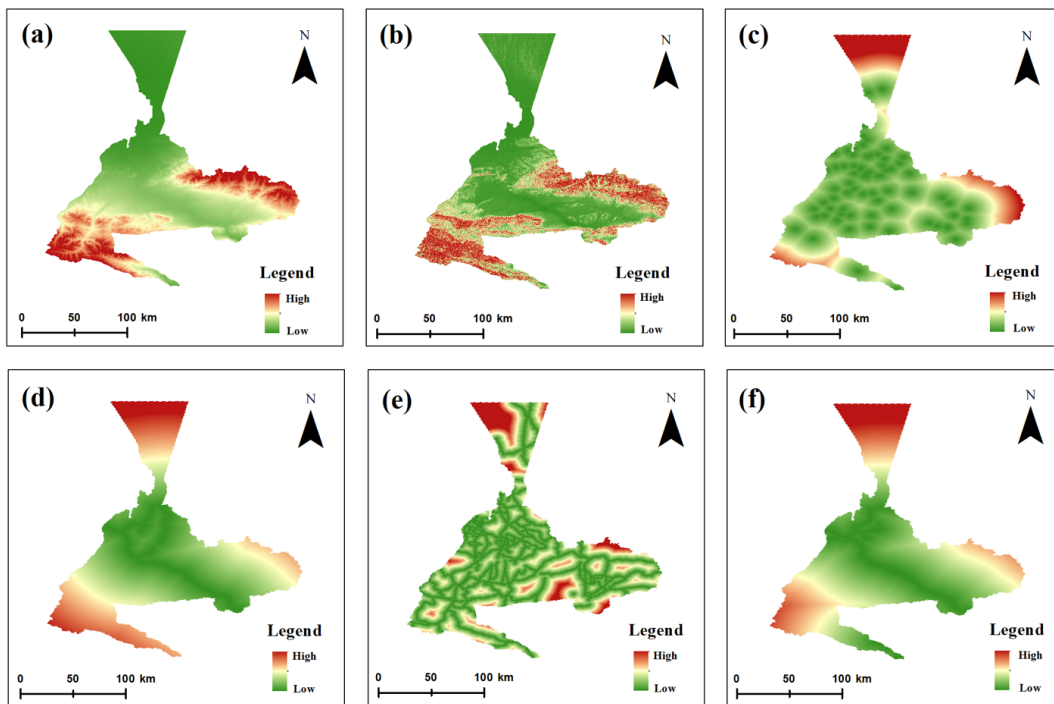


**Figure 2.** Factors driving land use changes in the study area including elevation (a), slope (b), proximity to human settlement (c), proximity to highway (d), proximity to other roads (e) and proximity to railroad (f).

2.5. Scenario Development

In this study, three scenarios were developed, namely the Baseline Scenario (BLS), Cultivated Land Protection Scenario (CPS) and Ecological Protection Scenario (EPS). The BLS assumes that the land use changes during 2020–2050 are not affected by policy interference to a large extent, and that the land use changes are consistent with that between 1980 and 2020. Based on the BLS, the CPS strictly controls the total amount of urban land, improves the land utilization rate and controls the conversion of cultivated land to urban land. EPS strengthens the protection of grassland and forest land and strictly controls the conversion of the grassland and forest land with ecological functions to construction land. Developing these three scenarios was based on parameterizing the transition cost matrix in the model. Cost matrix settings of three scenarios are shown in Table 1. In the cost matrix, 1 indicates that a land use type is allowed to be converted to another land use type, while 0 indicates that a land use type is not allowed to be converted to another land use type.

**Table 1.** The cost matrix of three scenarios.

Scenario Settings	BLS						CPS						EPS					
	CL	FL	GL	WB	UL	UnL	CL	FL	GL	WB	UL	UnL	CL	FL	GL	WB	UL	UnL
CL	1	1	1	0	1	0	1	0	0	0	0	0	1	1	1	0	1	0
FL	1	1	1	0	1	0	1	1	1	0	1	0	0	1	0	0	0	0
GL	1	1	1	0	1	0	1	1	1	0	1	0	0	1	1	1	0	0
WB	0	0	0	1	0	0	0	0	0	1	0	0	0	0	0	1	0	0
UL	1	1	1	1	1	1	1	1	1	1	1	1	1	1	1	1	1	1
UnL	1	1	1	1	1	0	1	1	1	1	1	0	1	1	1	1	1	0

Note: CL, FL, GL, WB, UL and UnL represent cultivated land, forest land, grassland, water bodies, urban land and unused land, respectively.

## 2.6. Kappa Coefficient and FoM

The kappa coefficient and *FoM* are the most frequently used and well known validation indices with reliable evaluation criteria and clear physical significance for assessing the accuracy of land use simulations [42,43]. The kappa coefficient can express the relationship between correct and incorrect simulations from the model and the actual situation [44]. The *FoM* expresses the agreement between the actual and simulated land use changes. The *FoM* ranges from 0 to 1; the higher the value is, the better the simulation results are. The mathematical expression can be written as [45,46]:

$$FoM = B / (A + B + C + D) \quad (7)$$

where *A* indicates the quantity of errors that the actual transformation took place but the simulation does not change; *B* indicates correct quantity where both the actual and the simulated transformation occur; *C* indicates quantity of inconsistency of simulated and actual changes; and *D* indicates the area where the actual transformation does not take place but the simulation does change. *D* also indicates the quantity of errors in which the actual transformation does not occur but the simulation changes.

## 2.7. Validation of FLUS Model

To validate the accuracy of the FLUS model for the simulation of future land use in Urumqi City, spatial patterning of land use in 2020 was simulated using the land use data for 2000 and 2010 as the initial data. The spatial distribution of the actual and simulated land use in 2020 in the study region is shown in Figure 3. The results showed that the simulated and actual land use patterns in 2020 were highly consistent. The simulated and actual land use maps were compared, and the kappa coefficient and *FoM* were calculated. The results showed that the kappa coefficient and *FoM* of the simulation results for 2020 were 0.87 and 0.114, respectively, indicating that the accuracy of the simulation is satisfactory. Therefore, the FLUS model can simulate the future land use in the study area with a high degree of accuracy.

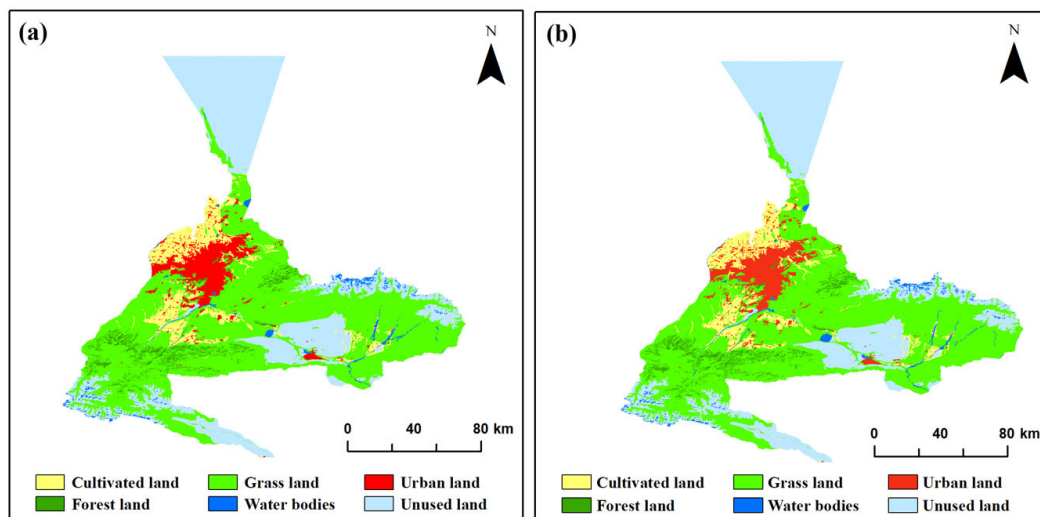


**Figure 3.** Actual land use pattern (a) and simulated land use pattern (b) in 2020.

## 3. Results and Discussion

### 3.1. LULC Change Analysis

Figure 4 and Tables 2 and 3 present the spatial distributions of the LULC classes and statistics of the areas between 1980 and 2020 in Urumqi City. The results showed that grassland was the major land use type, with the area accounting for more than 50%, followed by the unused land accounting for almost 30% of the study area. From 1980 to 2020, significant changes occurred in grassland and urban land. The urban land was

greatly expanded (530.76 km<sup>2</sup>) and urban expansion was rapid, whereas the grassland was decreased from 7903.4 km<sup>2</sup> to 7414.92 km<sup>2</sup>. The other land use types, including cultivated land, water bodies and unused land, decreased slightly with the changes of −1.14%, −0.95% and −0.70%, respectively, whereas forest land showed a slight increase (0.47%) from 1980 to 2020.

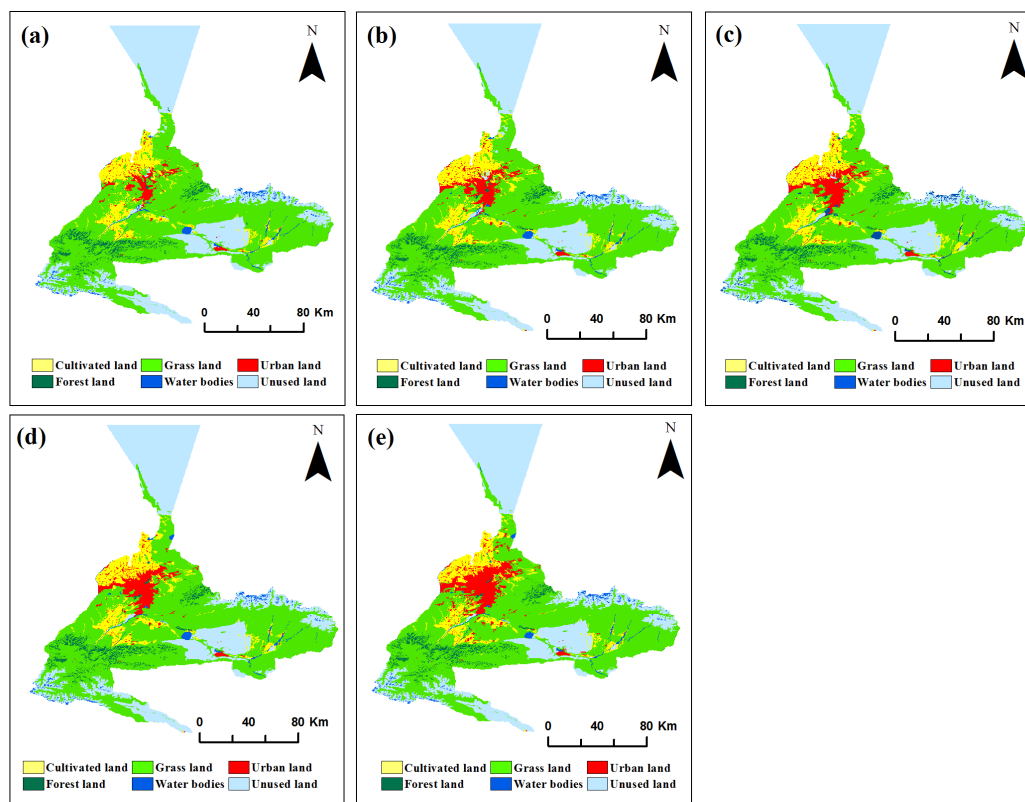


Figure 4. Land use map of the study area in 1980 (a), 1990 (b), 2000 (c), 2010 (d) and 2020 (e).

Table 2. LULC classes distribution of Urumqi City from 1980 to 2020.

Classes	1980		1990		2000		2010		2020	
	km <sup>2</sup>	%								
Cultivated land	1136.43	8.00	1219.55	8.59	1221.16	8.60	1235.15	8.70	1123.48	7.91
Forest land	405.02	2.85	414.78	2.92	402.41	2.83	408.84	2.88	406.91	2.87
Grassland	7903.4	55.65	7628.41	53.71	7589.62	53.44	7543.51	53.11	7414.92	52.21
Water bodies	222.66	1.57	222.69	1.57	234.75	1.65	229.59	1.62	220.55	1.55
Urban land	353.51	2.49	518.1	3.65	583.93	4.11	625.73	4.41	884.27	6.23
Unused land	4181.57	29.44	4199.06	29.57	4170.72	29.37	4159.77	29.29	4152.46	29.24

Table 3. The changes in area in km<sup>2</sup> of LULC from 1980 to 2020.

Classes	△1980–1990		△1990–2000		△2000–2010		△2010–2020	
	km <sup>2</sup>	%						
Cultivated land	83.12	7.31	1.61	0.13	13.99	1.15	−111.67	−9.04
Forest land	9.76	2.41	−12.37	−2.98	6.43	1.60	−1.93	−0.47
Grassland	−274.99	−3.48	−38.79	−0.51	−46.11	−0.61	−128.59	−1.70
Water bodies	0.03	0.01	12.06	5.42	−5.16	−2.20	−9.04	−3.94
Urban land	164.59	46.56	65.83	12.71	41.8	7.16	258.54	41.32
Unused land	17.49	0.42	−28.34	−0.67	−10.95	−0.26	−7.31	−0.18

Note: △—Change in area in km<sup>2</sup>.

The general trend of the LULC changes in the study region between 1980 and 2020 reveal that urban land increased consistently, and urban expansion was rapid. This result is consistent with fact that most Chinese cities experienced rapid urban expansion—especially after the “Reform and Opening-up” policy in 1970s, as reported by Zhang et al., who studied the urban expansion of 60 typical Chinese cities from 1970 to 2013 using remote sensing data [47]. Generally, urban expansion results from the various factors including natural and anthropogenic factors [48]. Natural factors mainly include topography and soil characteristics, which contribute to spatial heterogeneity. Anthropogenic factors include population growth and economic and urban transportation development [49]. Lin et al. studied the spatial changes and driving factors of land urbanization in 658 Chinese cities, and found that population growth, industrial development and investment rates were the major driving factors of land urbanization from 2000 to 2010 [50]. Wang and Lu studied the urban land expansion and driving factors of 55 Chinese mountain cities and identified that economic development, population growth, transportation development and urban development policy were the major driving forces of the urban land expansion. According to official statistical data, the total population of Urumqi increased from 1.19 million people to 2.22 million people between 1980 and 2018, while the total GDP of Urumqi increased from RMB 1.13 billion to RMB 309.98 billion from 1980 to 2018.

### 3.2. LULC Transitions

A Sankey diagram was used to illustrate the transitions between the different land use types presented in Figure 5. From 1980 to 1990, a notable share of grassland was converted into urban land and cultivated land with an area of 148 km<sup>2</sup> and 131.98 km<sup>2</sup>, respectively. Additionally, grassland was converted into unused land with an area of 29.67 km<sup>2</sup>, whereas cultivated land was converted into grassland with an area of 28.90 km<sup>2</sup>. No significant transitions were observed in the rest of the land use types between 1980 and 1990. From 1990 to 2000, fewer significant transitions were detected compared to the previous period. Cultivated land was converted into urban land with an area of 33.59 km<sup>2</sup>, whereas grassland was converted into cultivated land with an area of 27.58 km<sup>2</sup>. From 2000 to 2010, transitions between all land use types were not obvious. Grassland was converted into cultivated land and urban land with an area of 25.32 km<sup>2</sup> and 14.28 km<sup>2</sup>, respectively. Considerable transitions occurred between cultivated land, grassland and urban land between 2010 and 2020. Grassland was converted into urban land with an area of 154.80 km<sup>2</sup>, whereas cultivated land was converted into urban land and grassland with an area of 95.39 km<sup>2</sup> and 36.51 km<sup>2</sup>, respectively.

In summary, these results showed that significant transitions mainly occurred between grassland, cultivated land and urban land. Grassland and cultivated land have been converted into urban land, resulting in rapid urban expansion over the last 40 years. These results were consistent with the findings of Doe et al. [51], He et al. [52] and Lu et al. [53]. Tan et al. studied 145 major Chinese cities and found similar results—that urban land was expanded by 39.8%, with 70% of it being converted from cultivated land in the 1990s [54]. In addition, other negative impacts of rapid urban expansion have been reported in recent studies. Qi et al. investigated the positive and negative impacts of urban expansion on vegetation. They found that the negative impacts of urban expansion were much higher than the positive impacts [55]. Wei et al. assessed the relationship between urban expansion and habitat quality in 11 cities in China, and found that urban expansion was negatively correlated with habitat quality [56]. Wang et al. studied the impacts of urban land expansion on the regional environment of Yangon City and Nay Pyi Taw City in Burma and found that urban expansion led to an increase in land surface temperature, loss of tree cover and a decrease in net primary productivity [57].

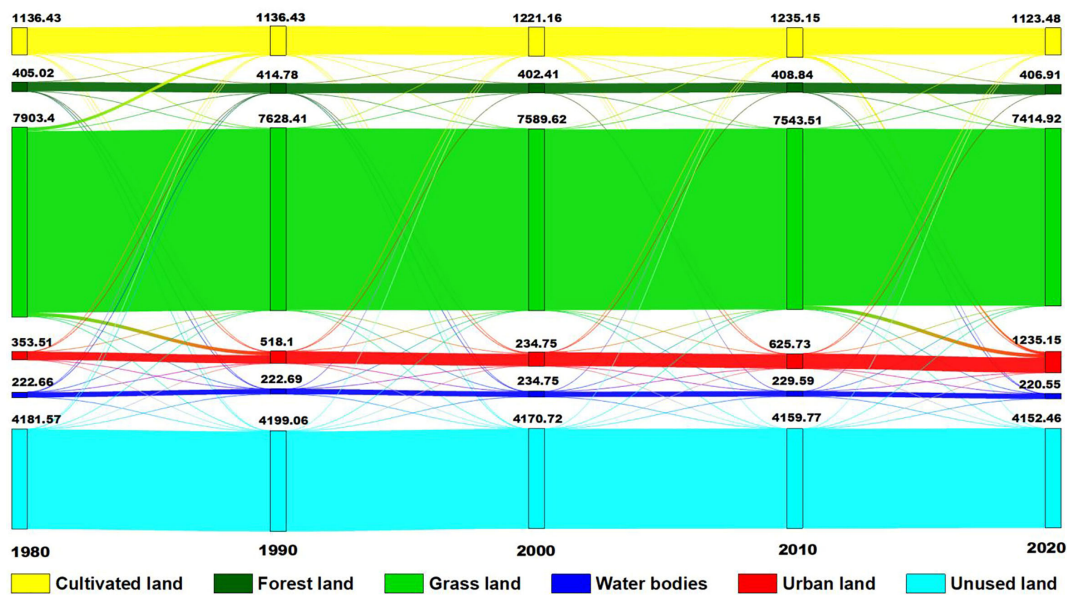


**Figure 5.** Sankey diagram of land use changes between types in Urumqi city from 1980 to 2020.

### 3.3. LUCC Future Predictions

To explore land use changes for 2030 and 2050, the FLUS model was applied to predict the spatial distribution of land use for 2030 and 2050 under different scenarios (Figures 6 and 7). Under the BLS, urban land was found to increase by 227.37 km<sup>2</sup> in 2030 and 614.55 km<sup>2</sup> in 2050, while unused land decreased by 35.39 km<sup>2</sup> in 2030 and 69.74 km<sup>2</sup> in 2050 compared to 2020. On the contrary, grassland was observed to decrease by 105.55 km<sup>2</sup> in 2030 and 335.20 km<sup>2</sup> in 2050, while cultivated land decreased by 89.58 km<sup>2</sup> in 2030 and 208.61 km<sup>2</sup> by 2050 compared to 2020. Additionally, the water bodies and forest land showed few changes in 2030 and 2050.

Under the CPS, major changes will occur in urban land and grassland by 2030 and 2050. The urban land increased by 121.10 km<sup>2</sup> in 2030 and 350.82 km<sup>2</sup> in 2050, while grassland decreased by 132.64 km<sup>2</sup> in 2030 and 350.82 km<sup>2</sup> in 2050 compared to 2020. Changes of other land use types, including cultivated land, forest land, water bodies and unused land, were not obvious. Moreover, the expansion rate of the urban land declined, while the area of cultivated land increased significantly compared with the BLS. This is mainly because the development of urban land will be constrained to a certain extent by the transfer and change restrictions of cultivated land to other land use types. In addition, grassland became a major source of urban expansion under the CPS.

Under the EPS, significant changes still occurred in urban land and cultivated land. Urban land was found to increase by 69.75 km<sup>2</sup> in 2030 and 187.16 km<sup>2</sup> in 2050, while the cultivated land showed a decreasing trend, and its area decreased by 89.61 km<sup>2</sup> in 2030 and 185.34 km<sup>2</sup> in 2050 compared to 2020. Compared to 2020, forest land increased by 32.90 km<sup>2</sup> and 32.24 km<sup>2</sup> in 2030 and 2050, and grassland decreased by 15.93 km<sup>2</sup> and 28.33 km<sup>2</sup> in 2030 and 2050. The results show that the expansion of urban land is obvious; however, the expansion rate is effectively controlled. Additionally, grassland and forest land were effectively protected compared to the other two scenarios.

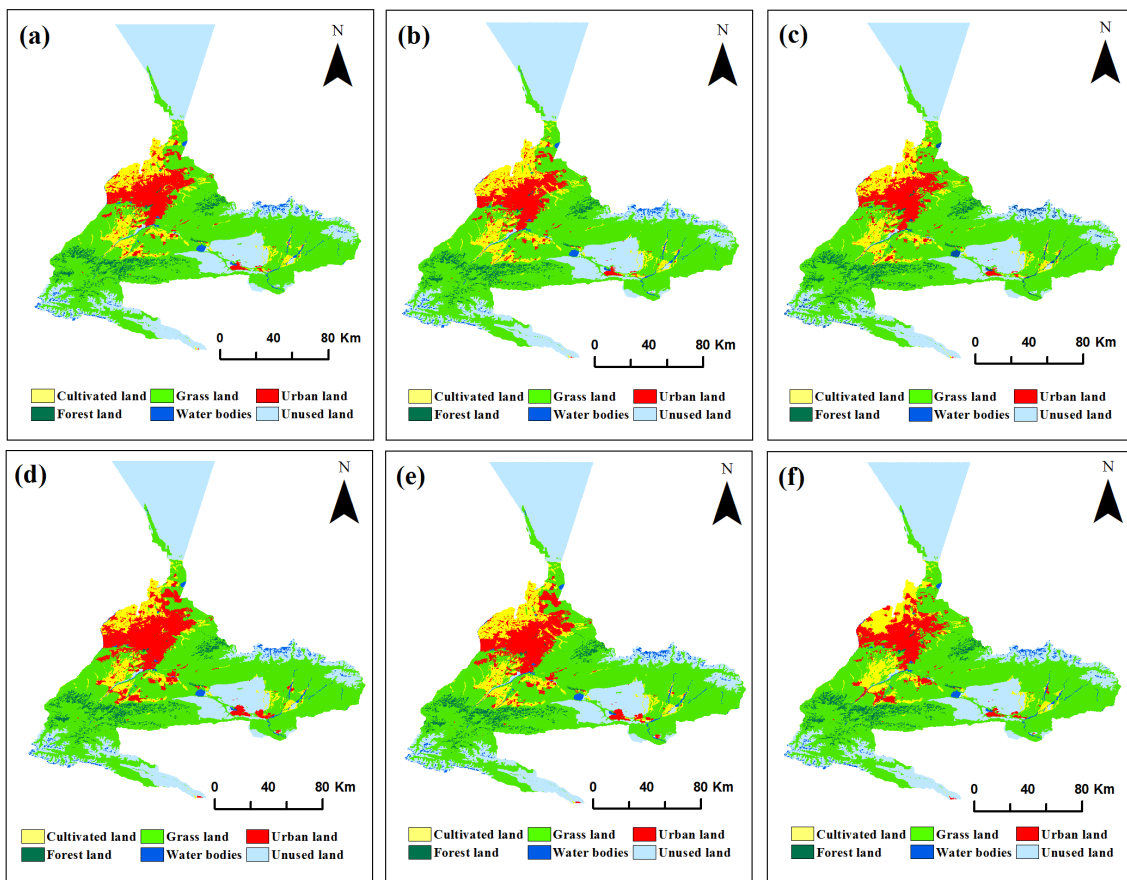


Figure 6. Spatial distribution of predicted land use in 2030 under BLS (a), CPS (b) and EPC (c) and in 2050 under BLS (d), CPS (e) and EPC (f).

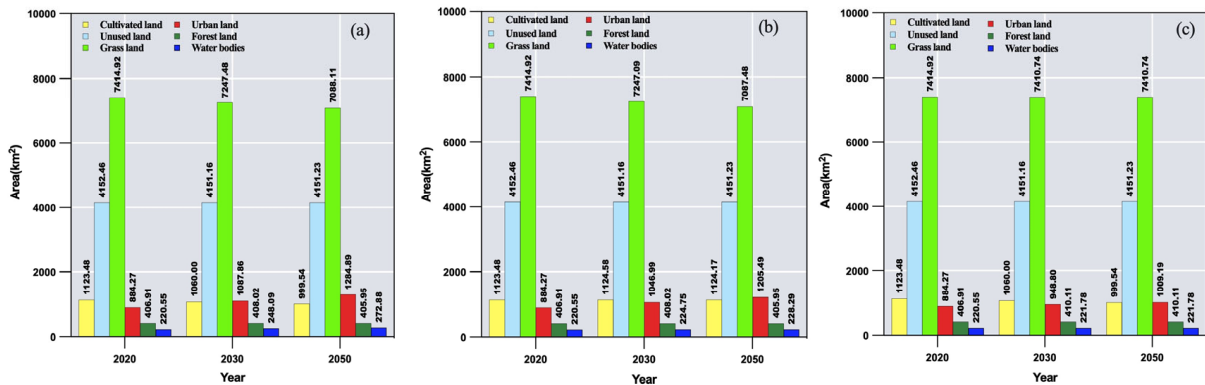


Figure 7. Predicted land use in 2030 and 2050 under BLS (a), CPS (b) and EPC (c).

In summary, urban land is expected to increase over the next 30 years under all three scenarios. Other land use types, including forest land, grassland, water bodies, unused land and cultivated land showed different change characteristics under different scenarios. These results are consistent with the findings of Liu et al. who studied the potential impacts of urban land use changes on supply and demand of water resources in Yulin city, Shanxi province, China [58]. Under the BLS, urban land will continue to expand, while the grassland and cultivated land will have a trend to decrease in 2030 and 2050 compared with in 2020. Such significant changes in land use may trigger a series of environmental problems, including an increase in the urban heat island effect and loss of the ecosystem services, as reported in other studies [59–64]. Additionally, the decline in cultivated land may have affected the self-sufficiency of agricultural products in the study area. Under

the CPS and the EPS, the expansion of urban land is obvious, but its expansion rate is effectively controlled compared with that of the BLS. In addition, cultivated land, grassland and forest land were effectively protected under the CPS and the EPS compared to the BLS.

Our research results revealed historical and future spatiotemporal patterns of LULC of Urumqi City, which was helpful for tracking the progress towards the United Nations' *Sustainable Development Goals* (SDGs), including the preservation of healthy ecosystems and the biological diversity supported by land resources (SDGs 12, 15), mitigation of the urban heat island effect caused by climate change (SDGs 13) and intensive and efficient use of urban land resources (SDGs 2, 9). In conclusion, decision makers may consider policy options including strictly protecting the cropland and grassland, limiting the disorderly urban expansion and developing an ecological economy-based society to achieve sustainable development and land use.

#### 4. Conclusions

This study assessed the spatiotemporal characteristics of LULC during the time intervals between 1980, 1990, 2000, 2010 and 2020. Moreover, future LULC was successfully projected for 2030 and 2050 under different scenarios based on the FLUS model. The results demonstrated that grassland was the major land use type, with the area accounting for more than 50% of the study area. From 1980 to 2020, urban land expanded significantly while grassland decreased significantly. In addition, significant transitions mainly occurred between grassland, cultivated land and urban land. Grassland and cultivated land have been converted into urban land resulting rapid urban expansion over the last 40 years. Finally, as per the simulation results of LULC, urban land is expected to increase under all three scenarios, and cultivated land, grassland and forest land are effectively protected under the CPS and the EPS, compared to the BLS. Therefore, it may be the feasible option to consider multiple policies to achieve sustainable land management and prevent environmental problems caused by the land use changes in this study area.

Future LULC was successfully projected for 2030 and 2050 under different scenarios, based on the FLUS model. The simulation accuracy was satisfactory according to the kappa coefficient and *FoM*. However, only six driving forces were considered in the simulation process. Some important socioeconomic and policy factors were not included because of data availability and spatial resolution. This may have an impact on the accuracy of predicting the future land use in Urumqi City. Therefore, more comprehensive driving factors, including gross domestic product (GDP) and population, etc., are needed to improve simulation accuracy of the FLUS model in the future research. In addition, climate change also has a great impact on LULC changes, especially in arid and semi-arid regions. Future work is required to evaluate how LULC changes under different climate change scenarios. Finally, many models and software packages are available and are widely used in future land use simulations, as described above. Future research should focus on comparing the simulation accuracy and differences of these models for predicting future LULC in arid and semi-arid regions.

**Author Contributions:** Conceptualization, Y.M. (Yusuyunjiang Mamitimin), Z.S., A.M., B.M. and Y.M. (Yunfei Ma); formal analysis, Y.M. (Yusuyunjiang Mamitimin); methodology, Y.M. (Yusuyunjiang Mamitimin); project administration, Z.S.; software, Y.M. (Yusuyunjiang Mamitimin); validation, Y.M. (Yusuyunjiang Mamitimin); visualization, Y.M. (Yusuyunjiang Mamitimin); writing—original draft, Y.M. (Yusuyunjiang Mamitimin); writing—review and editing, Y.M. (Yusuyunjiang Mamitimin), Z.S., A.M., B.M. and Y.M. (Yunfei Ma). All authors have read and agreed to the published version of the manuscript.

**Funding:** This research was funded by the National Natural Science Foundation of China (Grant No. 41661036) and the National Natural Science Foundation of China—Xinjiang Joint Fund (Grant No. U1603241).

**Institutional Review Board Statement:** Not applicable.

**Informed Consent Statement:** Not applicable.

**Data Availability Statement:** Not applicable.

**Acknowledgments:** We would like to thank National Natural Science Foundation of China for funding this research. We also would like to thank the anonymous reviewers for their constructive comments to improve the quality of this manuscript.

**Conflicts of Interest:** The authors declare no conflict of interest.

## References

1. Wang, Z.; Xu, X.; Wang, H.; Meng, S. Does land reserve system improve quality of urbanization? Evidence from China. *Habitat Int.* **2020**, *106*, 102291. [[CrossRef](#)]
2. United Nations Department of Economic and Social Affairs. *World Urbanization Prospects: The 2018 Revision*; United Nations: New York, NY, USA, 2019.
3. Chitonge, H.; Mfune, O. The urban land question in Africa: The case of urban land conflicts in the City of Lusaka, 100 years after its founding. *Habitat Int.* **2015**, *48*, 209–218. [[CrossRef](#)]
4. Liu, Y.; Fang, F.; Li, Y. Key issues of land use in China and implications for policy making. *Land Use Policy* **2014**, *40*, 6–12. [[CrossRef](#)]
5. Shan, L.; Yu, A.T.; Wu, Y. Strategies for risk management in urban–rural conflict: Two case studies of land acquisition in urbanising China. *Habitat Int.* **2017**, *59*, 90–100. [[CrossRef](#)] [[PubMed](#)]
6. Tafazzoli, M. Hydrologic responses to urbanization: Towards a holistic approach for maximizing green roofs' performance in controlling urban precipitations. *Urban Clim.* **2023**, *48*, 101352. [[CrossRef](#)]
7. Ariken, M.; Zhang, F.; Liu, K.; Fang, C.; Kung, H.T. Coupling Coordination Analysis of Urbanization and Eco-Environment in Yanqi Basin Based on Multi-Source Remote Sensing Data. *Ecol. Indic.* **2020**, *114*, 106331. [[CrossRef](#)]
8. Li, S.C.; Zhao, Z.Q.; Wang, Y.L. Urbanization Process and Effects of Natural Resource and Environment in China: Research Trends and Future Directions. *Prog. Geogr.* **2009**, *28*, 63–70.
9. Zheng, H.; Khan, Y.A.; Abbas, S.Z. Exploration on the Coordinated Development of Urbanization and the Eco-Environmental System in Central China. *Environ. Res.* **2022**, *204*, 112097. [[CrossRef](#)]
10. Regasa, M.; Nones, M.; Adeba, D. A Review on Land Use and Land Cover Change in Ethiopian Basins. *Land* **2021**, *10*, 585. [[CrossRef](#)]
11. Huang, D.; Huang, J.; Liu, T. Delimiting Urban Growth Boundaries Using the Clue-S Model with Village Administrative Boundaries. *Land Use Policy* **2019**, *82*, 422–435. [[CrossRef](#)]
12. Chasia, S.; Olang, L.O.; Sitoki, L. Modelling of land-use/cover change trajectories in a transboundary catchment of the Sio-Malaba-Malakisi Region in East Africa using the CLUE-s model. *Ecol. Model.* **2023**, *476*, 110256. [[CrossRef](#)]
13. Zhang, X.; Ren, W.; Peng, H. Urban land use change simulation and spatial responses of ecosystem service value under multiple scenarios: A case study of Wuhan, China. *Ecol. Indic.* **2022**, *144*, 109526. [[CrossRef](#)]
14. Zhou, T.; Yang, X.; Ke, X. Delimitation of Urban Growth Boundaries by Integratedly Incorporating Ecosystem Conservation, Cropland Protection and Urban Compactness. *Ecol. Model.* **2022**, *468*, 109963. [[CrossRef](#)]
15. Liang, X.; Guan, Q.; Clarke, K.C.; Liu, S.; Wang, B.; Yao, Y. Understanding the drivers of sustainable land expansion using a patch-generating land use simulation (PLUS) model: A case study in Wuhan, China. *Comput. Environ. Urban Syst.* **2021**, *85*, 101569. [[CrossRef](#)]
16. Wang, Z.; Li, X.; Mao, Y.; Li, L.; Wang, X.; Lin, Q. Dynamic simulation of land use change and assessment of carbon storage based on climate change scenarios at the city level: A case study of Bortala, China. *Ecol. Indic.* **2022**, *134*, 108499. [[CrossRef](#)]
17. Liu, P.; Hu, Y.; Jia, W. Land Use Optimization Research Based on Flus Model and Ecosystem Services—Setting Jinan City as an Example. *Urban Clim.* **2021**, *40*, 100984. [[CrossRef](#)]
18. Jin, H.; Li, H.; Lee, J.; Sun, W. Simulation Analysis of Rural Land Use Using Rate of Change Driven by Population and Economic Dynamics—A Case Study of Huangguashan Village in Chongqing, China. *Ecol. Model.* **2023**, *475*, 110204. [[CrossRef](#)]
19. Liu, X.; Wei, M.; Li, Z.; Zeng, J. Multi-Scenario Simulation of Urban Growth Boundaries with an Esp-Flus Model: A Case Study of the Min Delta Region, China. *Ecol. Indic.* **2022**, *135*, 108538. [[CrossRef](#)]
20. Fashae, O.A.; Tijani, M.N.; Adekoya, A.E.; Tijani, S.A.; Adagbasa, E.G.; Aladejana, J.A. Comparative Assessment of the Changing Pattern of Land Cover Along the Southwestern Coast of Nigeria Using Gis and Remote Sensing Techniques. *Sci. Afr.* **2022**, *17*, e01286. [[CrossRef](#)]
21. Fu, F.; Deng, S.; Wu, D.; Liu, W.; Bai, Z. Research on the Spatiotemporal Evolution of Land Use Landscape Pattern in a County Area Based on Ca-Markov Model. *Sustain. Cities Soc.* **2022**, *80*, 103760. [[CrossRef](#)]
22. Tariq, A.; Yan, J.; Mumtaz, F. Land Change Modeler and Ca-Markov Chain Analysis for Land Use Land Cover Change Using Satellite Data of Peshawar, Pakistan. *Phys. Chem. Earth A/B/C* **2022**, *128*, 103286. [[CrossRef](#)]
23. Ma, B.; Wang, X. What Is the Future of Ecological Space in Wuhan Metropolitan Area? A Multi-Scenario Simulation Based on Markov-Flus. *Ecol. Indic.* **2022**, *141*, 109124. [[CrossRef](#)]
24. Ma, Y.; Wang, M.; Zhou, M.; Tu, J.; Ma, C.; Li, S. Multiple Scenarios-Based on a Hybrid Economy–Environment–Ecology Model for Land-Use Structural and Spatial Optimization under Uncertainty: A Case Study in Wuhan, China. *Stoch. Environ. Res. Risk Assess.* **2022**, *36*, 2883–2906. [[CrossRef](#)]

25. Guo, H.; Cai, Y.; Li, B.; Tang, Y.; Qi, Z.; Huang, Y.; Yang, Z. An Integrated Modeling Approach for Ecological Risks Assessment under Multiple Scenarios in Guangzhou, China. *Ecol. Indic.* **2022**, *142*, 109270. [[CrossRef](#)]
26. Hu, X.; Li, Z.; Cai, Y.; Wu, F. Urban Construction Land Demand Prediction and Spatial Pattern Simulation under Carbon Peak and Neutrality Goals: A Case Study of Guangzhou, China. *J. Geogr. Sci.* **2022**, *32*, 2251–2270. [[CrossRef](#)]
27. Xiang, S.; Wang, Y.; Deng, H.; Yang, C.; Wang, Z.; Gao, M. Response and Multi-Scenario Prediction of Carbon Storage to Land Use/Cover Change in the Main Urban Area of Chongqing, China. *Ecol. Indic.* **2022**, *142*, 109205. [[CrossRef](#)]
28. Wang, D.; Yang, C.; Shao, L. The Spatiotemporal Evolution of Hydrochemical Characteristics and Groundwater Quality Assessment in Urumqi, Northwest China. *Arab. J. Geosci.* **2021**, *14*, 161. [[CrossRef](#)]
29. Tsagkis, P.; Bakogiannis, E.; Nikitas, A. Analysing Urban Growth Using Machine Learning and Open Data: An Artificial Neural Network Modelled Case Study of Five Greek Cities. *Sustain. Cities Soc.* **2023**, *89*, 104337. [[CrossRef](#)]
30. Devendran, A.A.; Gnanappazham, L. Comparison of Urban Growth Modeling Using Deep Belief and Neural Network Based Cellular Automata Model—A Case Study of Chennai Metropolitan Area, Tamil Nadu, India. *J. Geogr. Inf. Syst.* **2019**, *11*, 1–16.
31. Yang, X.; Zheng, X.-Q.; Chen, R. A Land Use Change Model: Integrating Landscape Pattern Indexes and Markov-Ca. *Ecol. Model.* **2014**, *283*, 1–7. [[CrossRef](#)]
32. Liping, C.; Sun, Y.; Sajjad, S.; Andreas, W.N. Monitoring and Predicting Land Use and Land Cover Changes Using Remote Sensing and Gis Techniques—A Case Study of a Hilly Area, Jiangle, China. *PLoS ONE* **2018**, *13*, e0200493. [[CrossRef](#)]
33. Al-Sharif, A.A.A.; Pradhan, B. Monitoring and Predicting Land Use Change in Tripoli Metropolitan City Using an Integrated Markov Chain and Cellular Automata Models in Gis. *Arab. J. Geosci.* **2014**, *7*, 4291–4301. [[CrossRef](#)]
34. Ye, B.; Bai, Z. Simulating Land Use/Cover Changes of Nenjiang County Based on Ca-Markov Model. *Int. Fed. Inf. Process. Publ. IFIP* **2008**, *258*, 321–329.
35. Gidey, E.; Dikinya, O.; Sebege, R.; Segosebe, E.; Zenebe, A. Cellular Automata and Markov Chain (Ca\_Markov) Model-Based Predictions of Future Land Use and Land Cover Scenarios (2015–2033) in Raya, Northern Ethiopia. *Model. Earth Syst. Environ.* **2017**, *3*, 1245–1262. [[CrossRef](#)]
36. Sang, L.; Zhang, C.; Yang, J.; Zhu, D.; Yun, W. Simulation of land use spatial pattern of towns and villages based on CA-Markov model. *Math. Comput. Model.* **2011**, *54*, 938–943. [[CrossRef](#)]
37. Gharaibeh, A.; Shaamala, A.; Obeidat, R.; Al-Kofahi, S. Improving land-use change modeling by integrating ANN with Cellular Automata-Markov Chain model. *Heliyon* **2020**, *6*, e05092. [[CrossRef](#)]
38. Guan, D.; Gao, W.; Watari, K.; Fukahori, H. Land use change of Kitakyushu based on landscape ecology and Markov model. *J. Geogr. Sci.* **2008**, *18*, 455–468. [[CrossRef](#)]
39. Yang, X.; Zheng, X.Q.; Lv, L.N. A Spatiotemporal Model of Land Use Change Based on Ant Colony Optimization, Markov Chain and Cellular Automata. *Ecol. Model.* **2012**, *233*, 11–19. [[CrossRef](#)]
40. Mondal, S.; Sharma, N.; Garg, P.; Kappas, M. Statistical Independence Test and Validation of Ca Markov Land Use Land Cover (Lulc) Prediction Results. *Egypt. J. Remote Sens. Space Sci.* **2016**, *19*, 259–272. [[CrossRef](#)]
41. Munthali, M.; Mustak, S.; Adeola, A.; Botai, J.; Singh, S.; Davis, N. Modelling Land Use and Land Cover Dynamics of Dedza District of Malawi Using Hybrid Cellular Automata and Markov Model. *Remote Sens. Appl. Soc. Environ.* **2020**, *17*, 100276. [[CrossRef](#)]
42. Pontius, R.G.; Millones, M. Death to Kappa: Birth of Quantity Disagreement and Allocation Disagreement for Accuracy Assessment. *Int. J. Remote Sens.* **2011**, *32*, 4407–4429. [[CrossRef](#)]
43. Camacho Olmedo, M.T.; García-Álvarez, D.; Gallardo, M.; Mas, J.F.; Paegelow, M.; Castillo-Santiago, M.Á.; Molinero-Parejo, R. Validation of Land Use Cover Maps: A Guideline. In *Land Use Cover Datasets and Validation Tools: Validation Practices with QGIS*; García-Álvarez, D., Camacho Olmedo, M.T., Paegelow, M., Mas, J.F., Eds.; Springer International Publishing: Cham, Switzerland, 2022; pp. 35–46.
44. Pinto, N.; Antunes, A.P.; Roca, J. Applicability and calibration of an irregular cellular automata model for land use change. *Comput. Environ. Urban Syst.* **2017**, *65*, 93–102. [[CrossRef](#)]
45. Xu, Q.; Zhu, A.-X.; Liu, J. Land-use change modeling with cellular automata using land natural evolution unit. *Catena* **2023**, *224*, 106998. [[CrossRef](#)]
46. Paegelow, M. Lucc Based Validation Indices: Figure of Merit, Producer’s Accuracy and User’s Accuracy. In *Geomatic Approaches for Modeling Land Change Scenarios*; Camacho Olmedo, M.T., Paegelow, M., Mas, J.F., Escobar, F., Eds.; Springer International Publishing: Cham, Switzerland, 2018; pp. 326–433.
47. Zhang, Z.; Wen, Q.; Liu, F.; Zhao, X.; Liu, B.; Xu, J.; Yi, L.; Hu, S.; Wang, X.; Zuo, L.; et al. Urban expansion in China and its effect on cultivated land before and after initiating “Reform and Open Policy”. *Sci. China Earth Sci.* **2016**, *59*, 1930–1945. [[CrossRef](#)]
48. Liu, Y.; Yue, W.; Fan, P. Spatial determinants of urban land conversion in large Chinese cities: A case of Hangzhou. *Environ. Plan. B: Plan. Des.* **2011**, *38*, 706–725. [[CrossRef](#)]
49. Wu, Y.; Li, S.; Yu, S. Monitoring urban expansion and its effects on land use and land cover changes in Guangzhou city, China. *Environ. Monit. Assess.* **2015**, *188*, 54. [[CrossRef](#)]
50. Lin, X.; Wang, Y.; Wang, S.; Wang, D. Spatial differences and driving forces of land urbanization in China. *J. Geogr. Sci.* **2015**, *25*, 545–558. [[CrossRef](#)]
51. Doe, B.; Amoako, C.; Adamtey, R. Spatial Expansion and Patterns of Land Use/Land Cover Changes around Accra, Ghana—Emerging Insights from Awutu Senya East Municipal Area. *Land Use Policy* **2022**, *112*, 105796. [[CrossRef](#)]

52. He, Y.; Xia, C.; Shao, Z.; Zhao, J. The Spatiotemporal Evolution and Prediction of Carbon Storage: A Case Study of Urban Agglomeration in China's Beijing-Tianjin-Hebei Region. *Land* **2022**, *11*, 858. [\[CrossRef\]](#)
53. Lu, L.; Qureshi, S.; Li, Q.; Chen, F.; Shu, L. Monitoring and projecting sustainable transitions in urban land use using remote sensing and scenario-based modelling in a coastal megacity. *Ocean Coast. Manag.* **2022**, *224*, 106201. [\[CrossRef\]](#)
54. Tan, M.; Li, X.; Lu, C. Urban land expansion and arable land loss of the major cities in China in the 1990s. *Sci. China Ser. D Earth Sci.* **2005**, *48*, 1492–1500. [\[CrossRef\]](#)
55. Qi, T.; Ren, Q.; Zhang, D.; Lu, W.; He, C. Impacts of urban expansion on vegetation in drylands: A multiscale analysis based on the vegetation disturbance index. *Ecol. Indic.* **2023**, *147*, 109984. [\[CrossRef\]](#)
56. Wei, L.; Zhou, L.; Sun, D.; Yuan, B.; Hu, F. Evaluating the impact of urban expansion on the habitat quality and constructing ecological security patterns: A case study of Jiziwan in the Yellow River Basin, China. *Ecol. Indic.* **2022**, *145*, 109544. [\[CrossRef\]](#)
57. Wang, C.; Myint, S.W.; Fan, P.; Stuhlmacher, M.; Yang, J. The impact of urban expansion on the regional environment in Myanmar: A case study of two capital cities. *Landsc. Ecol.* **2018**, *33*, 765–782. [\[CrossRef\]](#)
58. Liu, X.; Liu, Y.; Wang, Y.; Liu, Z. Evaluating potential impacts of land use changes on water supply–demand under multiple development scenarios in dryland region. *J. Hydrol.* **2022**, *610*, 127811. [\[CrossRef\]](#)
59. Moazzam, M.F.U.; Doh, Y.H.; Lee, B.G. Impact of urbanization on land surface temperature and surface urban heat Island using optical remote sensing data: A case study of Jeju Island, Republic of Korea. *Build. Environ.* **2022**, *222*, 109368. [\[CrossRef\]](#)
60. Chen, H.; Deng, Q.; Zhou, Z.; Ren, Z.; Shan, X. Influence of Land Cover Change on Spatio-Temporal Distribution of Urban Heat Island—A Case in Wuhan Main Urban Area. *Sustain. Cities Soc.* **2022**, *79*, 103715. [\[CrossRef\]](#)
61. Chen, S.; Haase, D.; Qureshi, S.; Firozjaei, M.K. Integrated Land Use and Urban Function Impacts on Land Surface Temperature: Implications on Urban Heat Mitigation in Berlin with Eight-Type Spaces. *Sustain. Cities Soc.* **2022**, *83*, 103944. [\[CrossRef\]](#)
62. Zhao, Y.; Wang, M.; Lan, T.; Xu, Z.; Wu, J.; Liu, Q.; Peng, J. Distinguishing the effects of land use policies on ecosystem services and their trade-offs based on multi-scenario simulations. *Appl. Geogr.* **2023**, *151*, 102864. [\[CrossRef\]](#)
63. Li, J.; Dong, S.; Li, Y.; Wang, Y.; Li, Z.; Li, F. Effects of Land Use Change on Ecosystem Services in the China–Mongolia–Russia Economic Corridor. *J. Clean. Prod.* **2022**, *360*, 132175. [\[CrossRef\]](#)
64. Maimaiti, B.; Chen, S.; Kasimu, A.; Simayi, Z.; Aierken, N. Urban spatial expansion and its impacts on ecosystem service value of typical oasis cities around Tarim Basin, northwest China. *Int. J. Appl. Earth Obs. Geoinf.* **2021**, *104*, 102554. [\[CrossRef\]](#)

**Disclaimer/Publisher's Note:** The statements, opinions and data contained in all publications are solely those of the individual author(s) and contributor(s) and not of MDPI and/or the editor(s). MDPI and/or the editor(s) disclaim responsibility for any injury to people or property resulting from any ideas, methods, instructions or products referred to in the content.